INTERNATIONAL JOURNAL FOR NUMERICAL METHODS IN FLUIDS
Int. J. Numer. Meth. Fluids 2004; **44**:1389–1404 (DOI: 10.1002/fld.676)

Effect of duct velocity profile and buoyancy-induced flow on efficiency of transient hydrodynamic removal of a contaminant from a cavity

Lih-chuan Fang*,†

Department of Mechanical Engineering, Chinese Military Academy, P.O. Box 90602-6, Fengshan, Kaohsiung 830, Taiwan, Republic of China

SUMMARY

This paper describes a preliminary numerical analysis of the effect of duct velocity profile and buoyancy-induced flow generated by the heat source on hydrodynamic removal of contaminants contained in cavities. The process of fluid renewal in a cavity is modelled via a numerical solution of the Navier–Stokes equations coupled with the energy equation for transient flows. The foulant has the same density as the fluid in the duct and the duct velocity profile is considered to be Poiseuille flow and Couette flow, respectively. The results show that the change in Grashof number and duct flow velocity profile causes a dramatic difference in the observed flow patterns and cleaning efficiency. From a cleaning perspective, the results suggest that Couette flow at higher value of Grashof number becomes more effective in further purging of contaminated fluid from a cavity. Copyright © 2004 John Wiley & Sons, Ltd.

KEY WORDS: laminar flow; numerical analysis; heat transfer; visualization; transient; mixed convection

1. INTRODUCTION

In the chemical and food processing industry, surfaces in vessels or pipe work are often fouled by the product or contaminant substance. This may cause a reduction in the performance of heat exchanger elements, increase in pressure losses and also result in adverse hygiene conditions arising. The quality and cleanliness of the processed material is maintained by periodically cleaning the ducts and pipelines. The most common means of cleaning is to flush the system with an appropriate fluid which may also be a solvent. In recent years, the hydrodynamic cleaning methodology to cleaning components, parts and pipelines has become widely accepted, since solvents used to clean a system can be environmentally harmful. In the past decade, several studies [1–3] have been reported which attempt to measure and

*Correspondence to: Lih-chuan Fang, Department of Information Management, Fooyin University, 151 Chinhsueh Road, Ta-Liao Hsiang, Kaohsiung Hsien 831, Taiwan, Republic of China.
†E-mail: sc086@mail.fy.edu.tw

Received 19 October 2002
Revised 18 August 2003

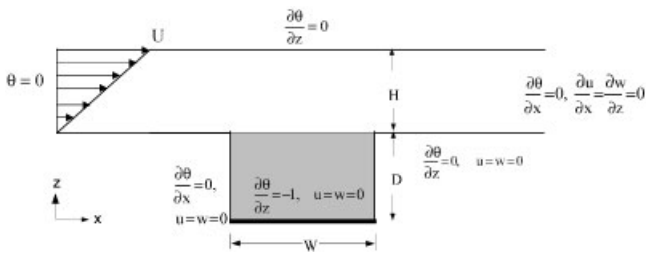

Figure 1. A sketch of the co-ordinate system in a duct with a rectangular cavity.

quantify the role of flow speed and surface geometry on the foulant which can be removed hydrodynamically. However, many of the foulants tested are real products which have been difficult to quantify, in that their viscosity, density and composition have not been measured. In addition, the variety of foulants in differing processes and geometries of the surface makes the study of the cleaning process more difficult; therefore most predictions of cleaning rates are empirical in nature. In consequence a starting point for such problems has been for the modelling of duct flow over a cavity.

Numerous studies of flow over cavities have been reported in the past few decades [4–9]. The results showed that the recirculation regions which may be observed in the problem of cavity cleaning are a function of cavity aspect ratio, relative duct size to cavity size and the parallel velocity within the duct. Recently, Fang *et al.* [10, 11] have presented a numerical and experimental study of the time-dependent hydrodynamic removal of a contaminated fluid from a cavity on the floor of a duct. It is shown that the cleaning of the foulant with the same density as the fluid in the duct or the heavier miscible foulant is more pronounced during the unsteady start-up of the duct flow and the rate of cleaning decreases as the flow reaches a steady state. The cleaning process is enhanced as the cavity aspect ratio (width/depth) is increased and as the duct Reynolds number increases. However, most studies to date have been concerned with the problem of Poiseuille flow over a cavity. Chilukrishna and Middleman [12] have pointed out that hydrodynamic cleaning of a surface frequently involves the use of a brush, squeezed mop or a rotating drum. In these situations the layer of fluid between the solid surface and applicator is quite small and the flow next to the surface can be considered as Couette flow. Some previous studies have focused on Couette flow over a cavity in which the upper wall of the duct is moved with a constant velocity, such as Mehta and Lavan [13], O'Brien [14] and Mickaily *et al.* [15]. They showed that there is a slightly different dividing streamline and cavity flow pattern between Poiseuille flow and Couette flow. Hence, it is of interest to know how the foulant is removed in Couette flow and how it might differ from Poiseuille flow.

The applications of convective heat transfer problems can be found numerously in science and engineering. In recent years, the studies on natural convective flow in a partially open enclosure have received considerable attention. Many authors have reported their studies on this problem including Oberkampf and Crow [16], Sparrow and Samie [17], Cha and Jaluria [18], Oosthuizen and Paul [19], Papanicolaou and Jaluria [20]. They pointed out that convective heat transfer in a partially open cavity causes a dramatic difference in the recirculation cavity flow and thermal field. The most recent work, Fang [21] investigated the effect of mixed

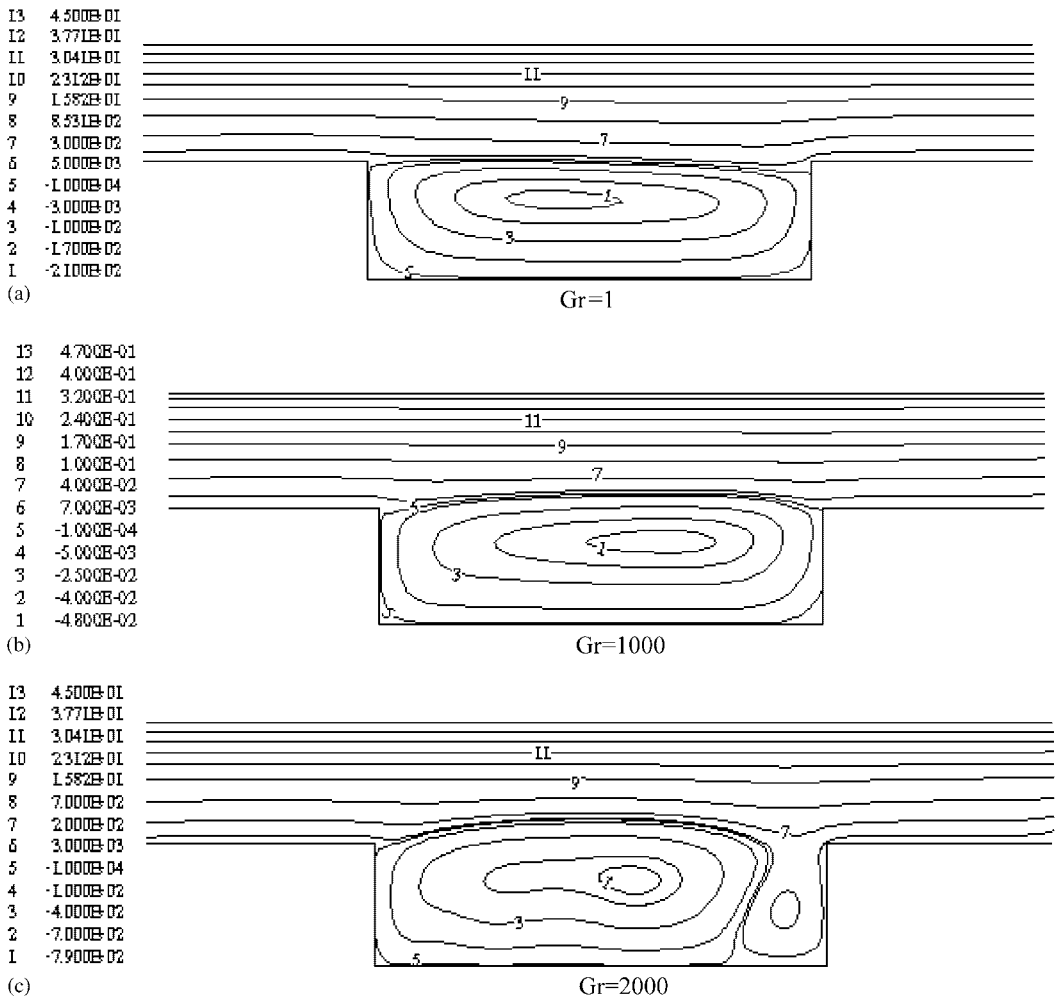

Figure 2. Streamlines of Couette flow over cavities with varied Grashof numbers, AR = 4 and $Re = 50$ at steady state.

convection on the problem of transient hydrodynamic removal of a contaminated fluid from a cavity. His results showed that the change in Grashof number causes a dramatic difference in the observed flow patterns and cleaning efficiency. The cleaning process is enhanced as Grashof number is increased due to the interaction between the external duct flow and buoyancy-induced flow arising from a thermal source. However, most studies to date have been concerned with the problem of Poiseuille flow over a cavity. Torrance *et al.* [22] presented numerical results for flow in a cavity with a moving upper wall. Their results showed that the flow patterns have tremendously changed for large Grashof numbers. Hence, it is of interest to know how the foulant is removed in Couette flow and how it might differ from Poiseuille flow under the effect of mixed convection.

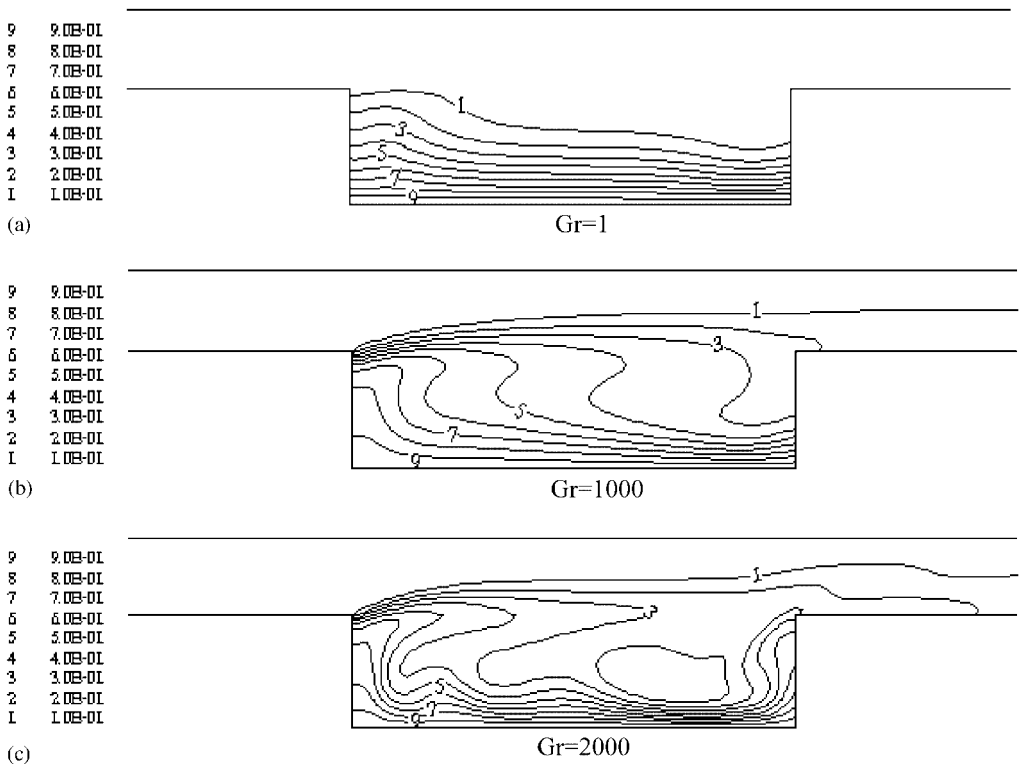

Figure 3. Isotherms of Couette flow over cavities with varied Grashof numbers, AR = 4, and $Re = 50$ at steady state.

Attention in the present work is focused on the effects of duct velocity profile and mixed convection on transient hydrodynamic removal of a contaminant from a cavity. The present work covers a wide range of Grashof numbers, Reynolds numbers and cavity aspect ratios with respect to the cleaning rate in laminar regime. In addition, the duct velocity profile is considered to be Poiseuille flow and Couette flow, respectively. The process of fluid renewal in a cavity is modelled via a numerical solution of the Navier–Stokes equations coupled with the energy equation for transient flows. The numerical method used is based on the MAC (Marker and Cell) method of Harlow and Welch [23]. Passive markers are used to visualize the flow and to quantify the hydrodynamic cleaning of the cavities.

2. PHYSICAL MODEL AND NUMERICAL METHOD

The problem schematic of the duct-cavity configuration employed in this study is shown in Figure 1. A Cartesian co-ordinate system is used with origin at the lower left hand corner of the computational domain. The cavity dimensions are defined by width W and depth D. Fluid of density ρ and viscosity μ flows continuously into the duct from the left and exits on the

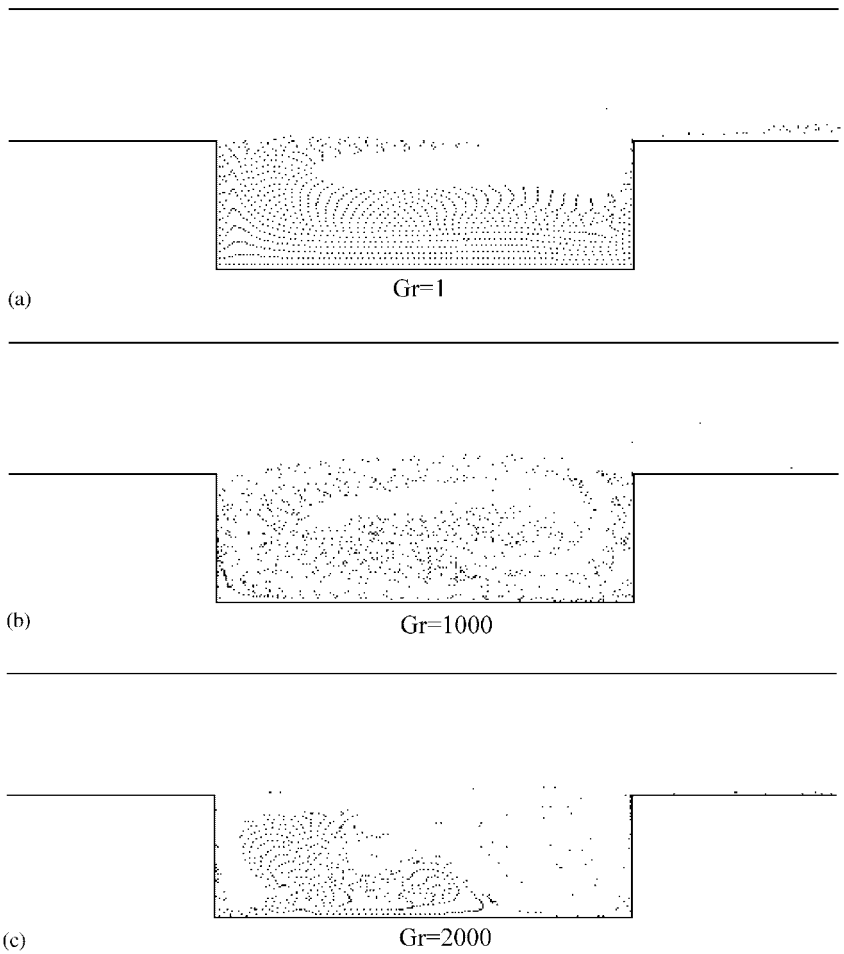

Figure 4. Flow evolution of Couette flow in a cavity of AR = 4 by using markers, for various Grashof numbers and $Re = 50$.

right. The acceleration, due to gravity g, acts in the negative z-direction. There is a constant-flux heat source q_s on the bottom wall of the cavity. All solid boundaries are assumed to be rigid no-slip walls. The height of the duct H was kept constant.

The fundamental non-dimensional equations in Cartesian form for two-dimensional incompressible flow of a Newtonian fluid with constant properties are

$$\frac{\partial u}{\partial x} + \frac{\partial w}{\partial z} = 0 \tag{1}$$

$$\frac{\partial u}{\partial t} + \frac{\partial u^2}{\partial x} + \frac{\partial uw}{\partial z} = -\frac{\partial p}{\partial x} + \frac{1}{Re}\left(\frac{\partial^2 u}{\partial x^2} + \frac{\partial^2 u}{\partial z^2}\right) \tag{2}$$

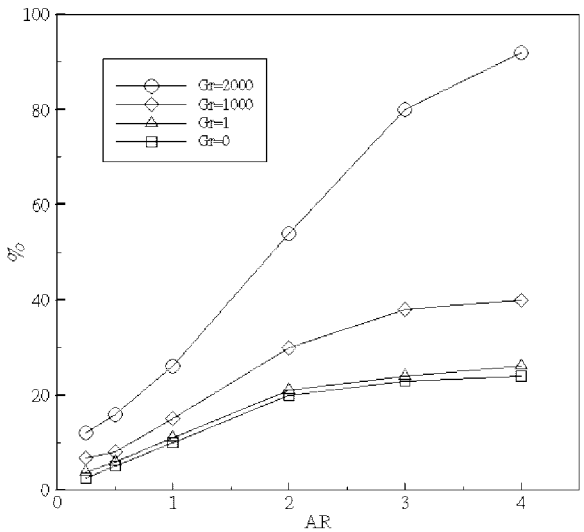

Figure 5. Percentage of markers removed from the cavity for varied Grashof numbers and $Re = 50$.

$$\frac{\partial w}{\partial t} + \frac{\partial wu}{\partial x} + \frac{\partial w^2}{\partial z} = -\frac{\partial p}{\partial z} + \frac{1}{Re}\left(\frac{\partial^2 w}{\partial x^2} + \frac{\partial^2 w}{\partial z^2}\right) + \frac{Gr}{Re^2}\,\theta \tag{3}$$

$$\frac{\partial \theta}{\partial t} + \frac{\partial u\theta}{\partial x} + \frac{\partial w\theta}{\partial z} = \frac{1}{Re\,Pr}\left(\frac{\partial^2 \theta}{\partial x^2} + \frac{\partial^2 \theta}{\partial z^2}\right) \tag{4}$$

where x and z are the dimensionless distances in the horizontal and the vertical directions, t is the dimensionless time, u and w are the dimensionless velocity components in the horizontal and the vertical directions, p is the dimensionless pressure and θ is the dimensionless temperature. The duct height H is chosen as the characteristic length, the maximum velocity of duct flow U as the characteristic velocity, the quantity ρU^2 as the characteristic pressure, and $q_s H/k$ as the characteristic temperature. The Reynolds number Re, the Grashof number Gr and the Prandtl number Pr are defined as

$$Re = \frac{UH}{v}, \quad Gr = \frac{g\beta\Delta T H^3}{v^2}, \quad Pr = \frac{v}{\alpha}$$

where α is the thermal diffusivity, β is the volumetric expansion coefficient, v is the kinematic viscosity and ΔT is set equal to $q_s H/k$.

The flow field is discretized into cells of size $\delta x \times \delta z$ with cell centres being designated by indices i in the x direction and k in the z direction. The u values are located on the vertical sides of the cell, and w values on the horizontal upper and lower sides. The values of p and θ are located at the cell centres. The Navier–Stokes equations and energy equation are represented in a finite-difference form by forward differencing in time and central differencing in space, except for the convection terms in the Navier–Stokes equations, where a combination of central and upstream differencing as described by Miyata and Nishimura [24] is used.

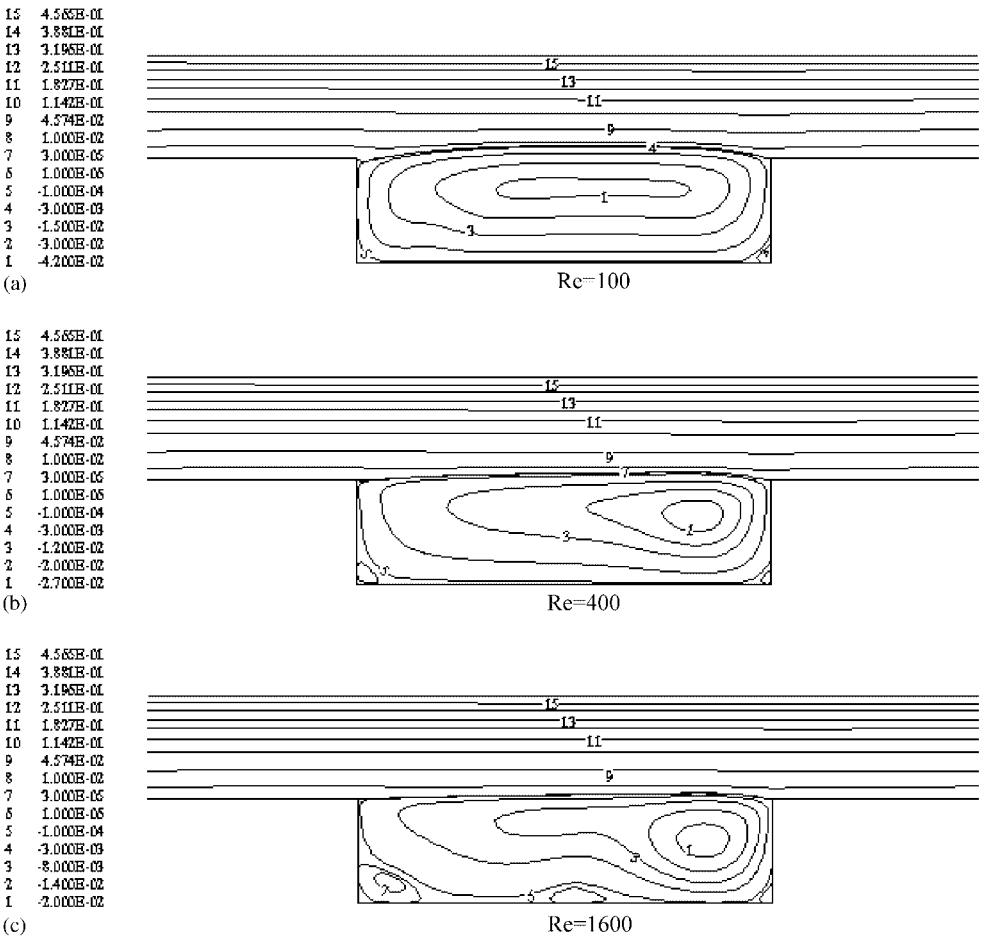

Figure 6. Streamlines of Couette flow over a cavity of AR = 4.0 for varied Reynolds numbers at $Gr = 2000$.

The solution is approached through the artificial compressibility method of Chorin [25] which involves a simultaneous iteration on pressure and velocity component. If $D_{i,k}^{n+1}$ represents the divergence of the fluid in a cell, where

$$D_{i,k}^{n+1} = \frac{1}{\delta x}(u_{i+1/2,k}^{n+1} - u_{i-1/2,k}^{n+1}) + \frac{1}{\delta z}(w_{i,k+1/2}^{n+1} - w_{i,k-1/2}^{n+1}) \tag{5}$$

then the pressure in cell i,k is updated through

$$(p_{i,k}^{n+1})^{m+1} = (p_{i,k}^{n+1})^{m} - R_f(D_{i,k}^{n+1})^{m} \tag{6}$$

where m indicates the mth iteration and R_f is a relaxation parameter. The solution is reached when the magnitude of $D_{i,k}^{n+1}$ in each cell is less than some pre-set small value, typically $O(10^{-6})$. The stability restriction is given by $R_f \leqslant \rho\delta x^2/2\delta t$ [26]. The optimum value of R_f

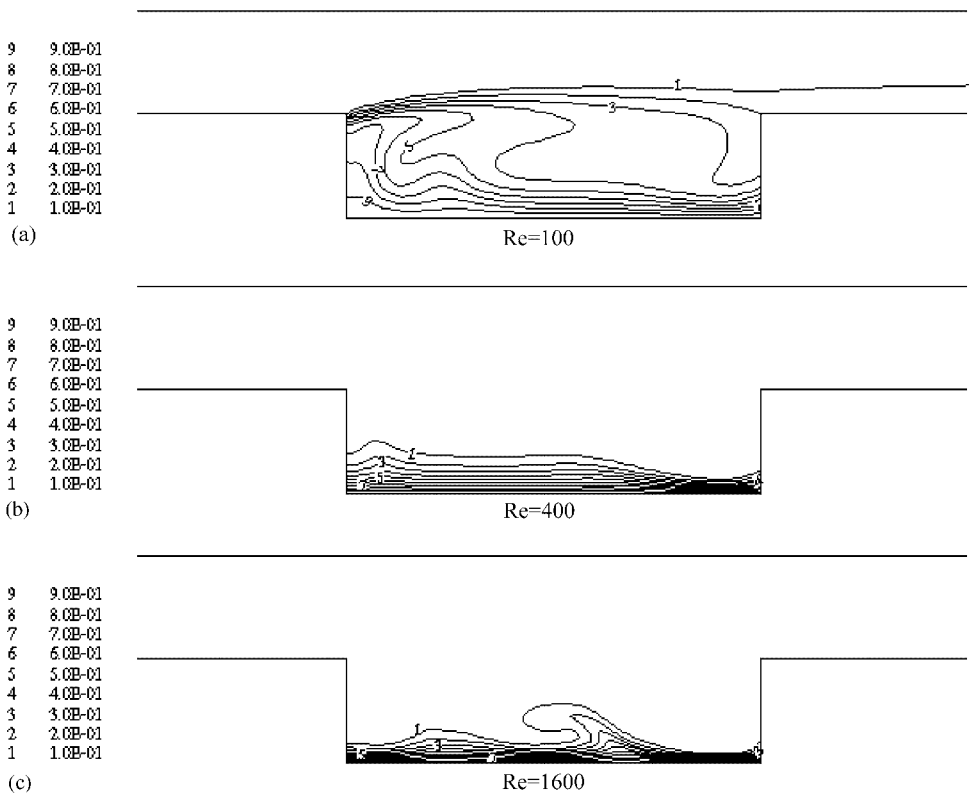

Figure 7. Isotherms of Couette flow over a cavity of AR = 4.0 for varied Reynolds numbers at $Gr = 2000$.

giving the most rapid convergence can, in general, only be determined by experimentation. Usually it is around $R_f = 1.8$.

In original MAC method, the energy equation is solved by a time-marching explicit method. Kuo *et al.* [27] have reported that an explicit method may lead to non-physical results in the transient solution. Thus, an implicit method is used to solve the energy equation in the present study. Therefore, there are two iterative processes in each time step to solve the pressure and velocity as well as temperature.

Boundary conditions are those appropriate to impermeable no-slip wall except at the upper moving wall where a flow velocity is prescribed at the upper wall and zero normal gradients are used to set variables just outside the outflow boundary. The boundary conditions for the temperature is $\theta = 0$ at the inflow boundary. The insulated conditions are imposed at the wall and at outflow as well, while $\partial\theta/\partial z = -1$ is specified at the bottom of the cavity. For the problem of a duct flow over a cavity the maximum cell size used was 0.02×0.02 and the time step never exceeded $\delta t = 0.01$ for the range of Reynolds numbers considered. Values less than these had negligible effect on the overall results obtained, but smaller cell sizes did improve the resolution of the smaller vortices in the cavities.

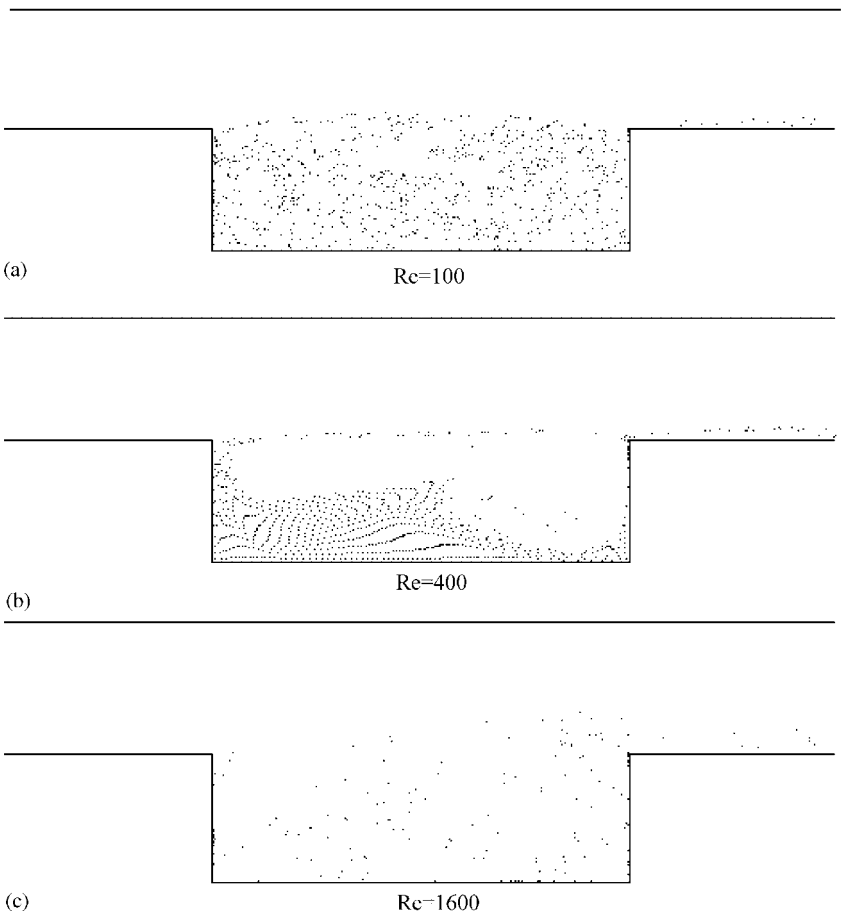

Figure 8. Flow evolution of Couette flow over a cavity of AR = 4 by using markers, for various Reynolds numbers at $Gr = 2000$.

Flow visualization and fluid contamination calculations are made possible by the use of passive markers. These are initially distributed before start-up and are moved to new positions at each time step. For example the new x-position of a marker k at time level $n+1$ is calculated from $x_k^{n+1} = x_k^n + u_k^{n+1}\delta t$ where u_k is the horizontal velocity at the marker position, x_k^n, and δt is a time step. The velocity components at the marker positions are calculated by a weighted interpolation of velocities in surrounding cells as described by Welch *et al.* [28].

The computer code has been validated by application to the problem for which solutions are available. The test was with mixed convection from an isolated heat source in a rectangular enclosure when $Re = 100$ and $Gr = 10\,000$ as considered by Papanicolaou and Jaluria [20]. The good agreement was obtained and given by Fang [21].

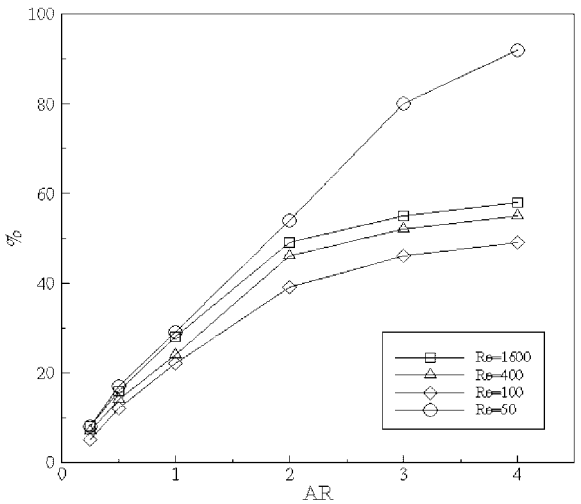

Figure 9. Percentage of markers removed from the cavity for varied Reynolds numbers at $Gr = 2000$.

3. RESULTS AND DISCUSSION

Although for the higher renewal rate of the cavities, the duct flow may be characterized by a turbulent regime, the present study is limited to the laminar regime as a first step. The present investigation covers a range of Grashof numbers, $Gr = 1$–2000, and a range of cavity aspect ratios, $\mathrm{AR} = 0.25$–4. A Prandtl number typical of water was assumed, $Pr = 7$. The flow is always considered to be laminar and the foulant has the same density as the fluid in the duct. In addition, the duct velocity profile is considered to be Poiseuille flow and Couette flow, respectively. The present study is concerned with the cleaning rate of contaminated fluid out from the cavity on the cleaning process and the previous work [10] have shown that no further removal of contaminant occurs after the steady-state vortex system becomes established. Hence, all the figures of the results are shown in steady state.

The case of Couette flow corresponds to the upper wall moving across the cavity from left to right at a constant speed U. For streamlines of Couette flow over a cavity of $\mathrm{AR} = 4.0$ and $Re = 50$ with various Grashof numbers, shown in Figure 2, it is seen that an increase in Grashof number results in the centre vortex moving downstream as Gr is less than 1000. There is a tremendous change in the flow pattern as $Gr = 2000$. The pronounced difference in the flow structure is that one small vortex is formed in the cavity. As the value of Gr greater than 2000, oscillatory behaviour was observed and the steady-state result could not be obtained. At such large value, small disturbances in the flow and a transition process to turbulent flow take place. Thus, $Gr = 2000$ is selected as the maximum Grashof number in the present study. It is also observed that the dividing streamline can bulge out into the duct as $Gr \geqslant 1000$. The isotherms varied with Grashof number are shown in Figure 3. For $Gr \geqslant 1000$, most of the area of the cavity remains the high temperature due to strong buoyancy. It is seen that as Grashof number increases the buoyancy enhances heat transfer.

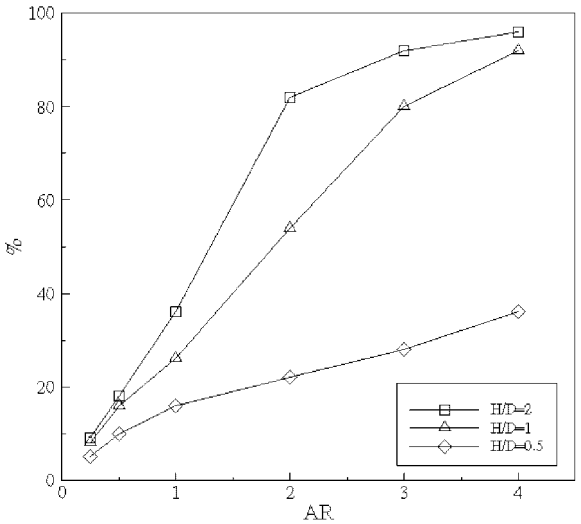

Figure 10. Percentage of markers removed from the cavity for varied H/Ds at $Gr = 2000$ and $Re = 50$.

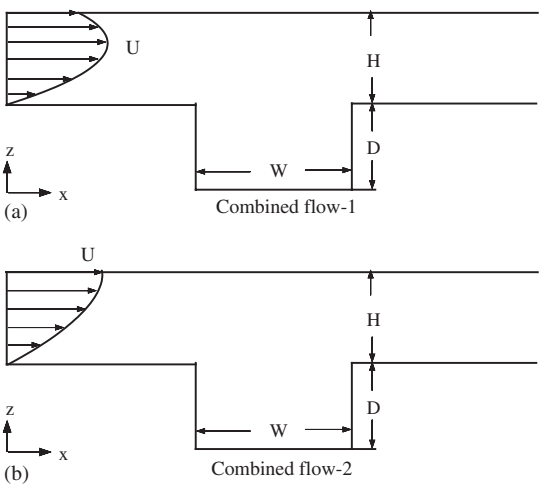

Figure 11. A sketch of the co-ordinate system for combined duct flow over a cavity: (a) Combined flow-1. (b) Combined flow-2.

The distribution of markers remaining in the cavity with various Grashof numbers at steady state is shown in Figure 4. It is worth mentioning that more markers are removed from the cavity as the Grashof number increases. In general, for Couette duct flow without the effect of mixed convection, the foulant is effectively trapped in the cavity. On the contrary, Couette flow under the strong buoyancy-induced flow generated by the heat source is effective in flushing out a cavity. A maximum of about 92% markers can be removed from the cavity as $AR = 4$ and $Gr = 2000$, shown in Figure 5.

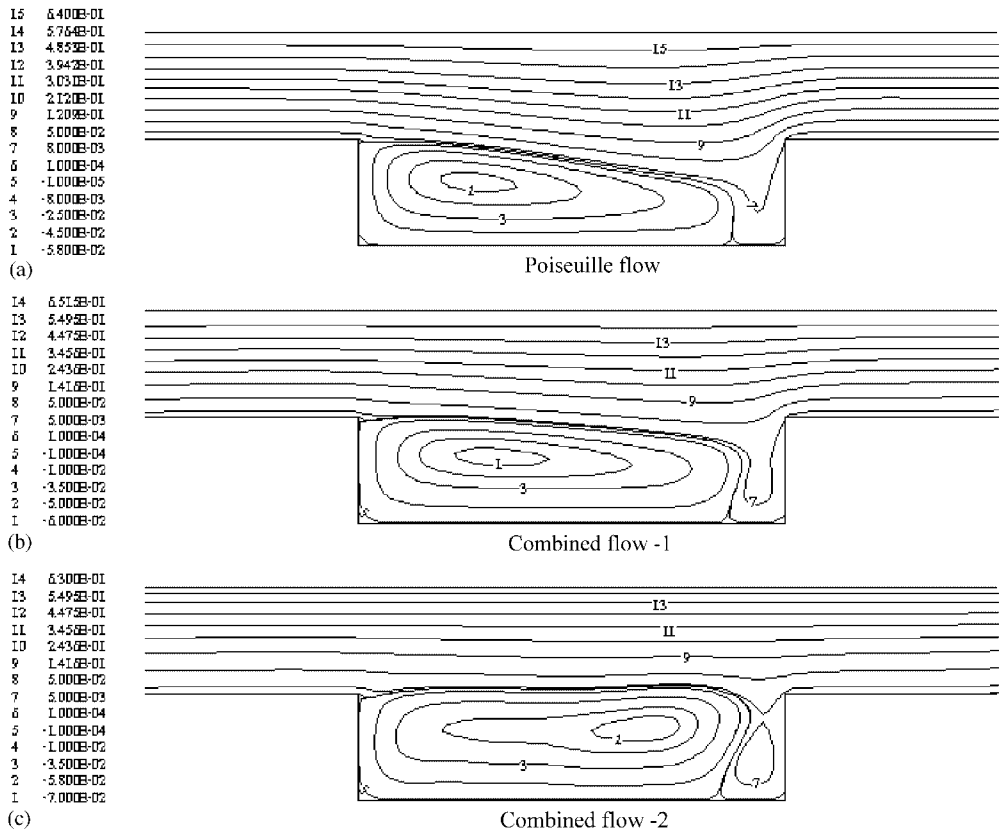

Figure 12. Streamlines of duct flow over cavities with aspect ratio of 4.0 and $Gr = 2000$, at $Re = 50$, for (a) Poiseuille flow, (b) combined flow-1, (c) combined flow-2.

The streamlines for the solutions at various values of Re while keeping Gr fixed at $Gr = 2000$ shown in Figure 6. It is seen that the large centre vortex fills the cavity as $Re = 100$. For the value of Re larger than 400, the centre vortex shifts to the far right side of the cavity. It can be seen that for $Re = 1600$ and values of Gr higher than 2000 the steady-state result could not be obtained, since oscillatory behaviour was observed. For lower Reynolds number $Re \leqslant 100$, the isotherm in Figure 7 shows that a large area of the cavity remains at higher temperature. The area of low temperature increases with the increase of Reynolds number. The main reason is that the buoyancy effect becomes insignificant while the region affected by the heat source becomes smaller due to the strong external flow. The distribution of markers remaining in the cavity, shown in Figure 8, matches the general distribution expected by observing the streamline patterns shown in Figure 6. It is interested to mention that the removal of markers increases as Reynolds number increases except for lower Reynolds number $Re = 50$, shown in Figure 9. It is obvious that due to the weak external flow at lower Reynolds numbers the strong buoyancy dominates the renewal process in the cavity. In addition, the effect of duct height H on cavity fluid removal as a function of cavity depth is investigated

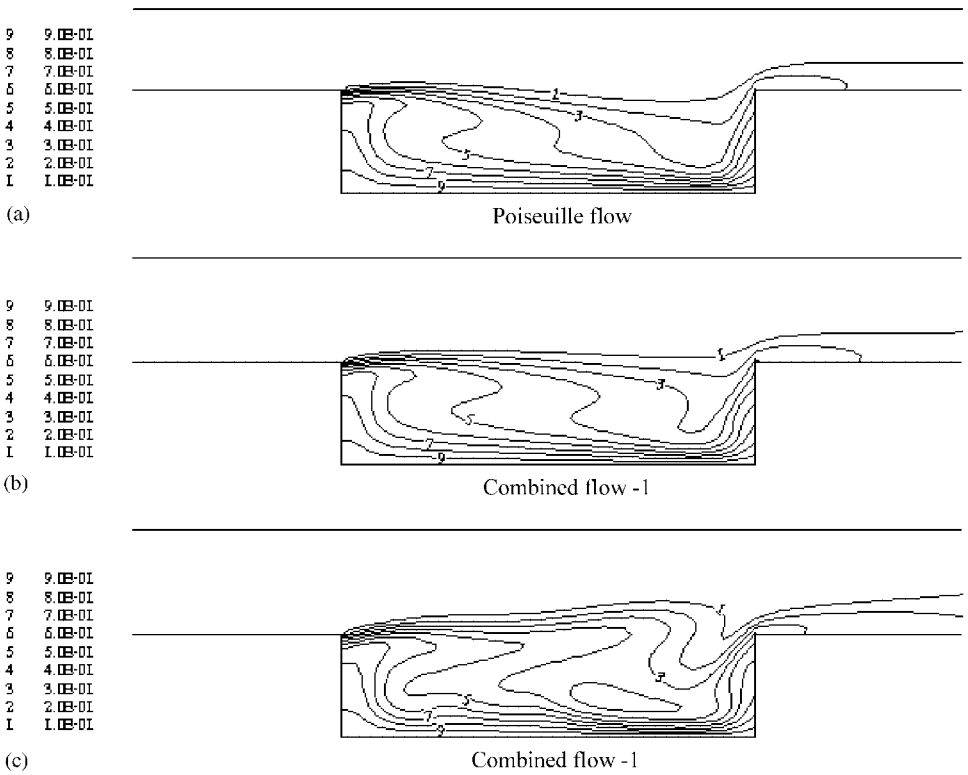

Figure 13. Isotherms of duct flow over cavities with aspect ratio of 4.0 and $Gr = 2000$, at $Re = 50$, for (a) Poiseuille flow, (b) combined flow-1, (c) combined flow-2.

in the present study. This means that the duct height is small compared to the cavity depth as the value of H/D decreases. It is obtained that the percentage of markers removed from a cavity increases with the increasing H/D, shown in Figure 10.

O'Brien [14] and Mickaily *et al.* [15] have studied the situation where a combination of Couette and Poiseuille flows is used under Stokes flow conditions. In this case, the upper wall moves at a velocity u from left to right and an existing Poiseuille flow acts in the same direction. Figure 11(a) shows a schematic diagram for when Poiseuille flow dominates, and 11(b) for when Couette flow dominates. The calculations with different input duct flows show that the closed flow within a given cavity depends upon the duct flow approaching the cavity. Figure 12 shows that the flow characteristics for the 'combined' inputs are intermediate between the individual Poiseuille and Couette flows over the cavity. The results in the present study show similar qualitative behaviour to those [14, 15] for Stokes flow. It is worth mentioning that for Poiseuille flow oscillatory behaviour at $Gr = 2000$ is not observed until the values of Gr higher than 4000 [21]. The isotherms and the distribution of markers remaining in the cavity are shown in Figures 13 and 14, respectively. The quantity of removal of markers is also intermediate between the individual Poiseuille and Couette flow cases and the results are shown in Figure 15. For Couette duct flow without the effect of mixed convection,

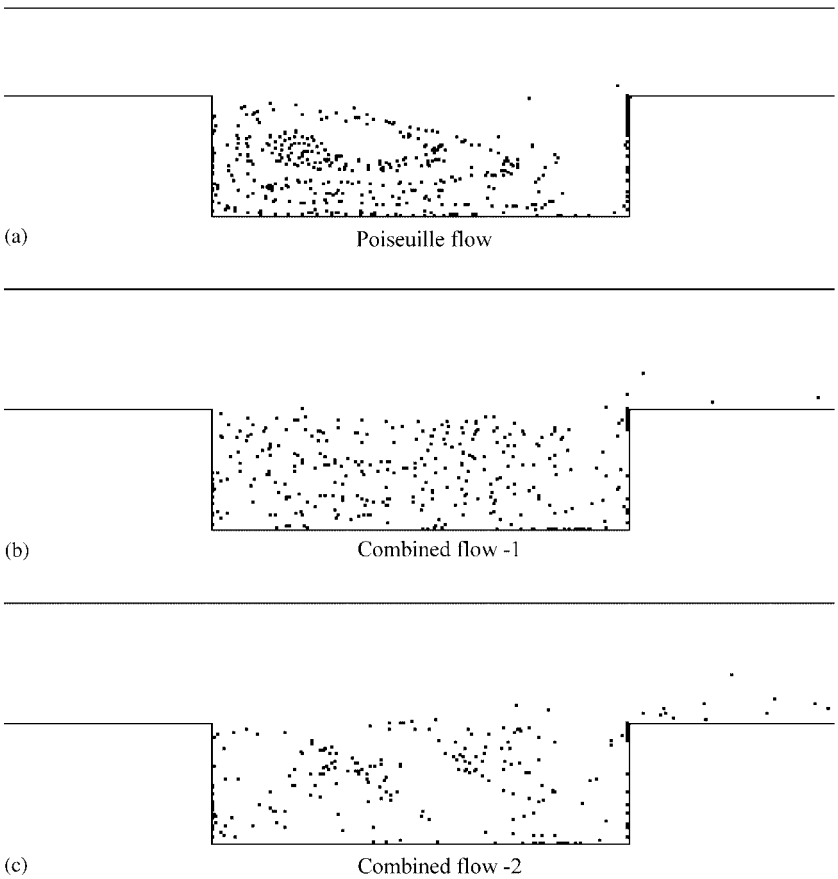

Figure 14. Flow evolution of duct flow over cavities with aspect ratio of 4.0 and $Gr = 2000$, at $Re = 50$, for (a) Poiseuille flow, (b) combined flow-1, (c) combined flow-2.

the previous results [11] show that the foulant is effectively trapped in the cavity and the cleaning process becomes overall less effective than Poiseuille duct flow. However, it can be seen from the present results that Couette flow at higher value of Gr and aspect ratio is more effective than Poiseuille flow for cleaning cavities.

4. CONCLUSIONS

Numerical analyses have been carried out to investigate the effect of duct velocity profile and buoyancy-induced flow on transient hydrodynamic cleaning of a rectangular cavity. The results show that the change in Grashof number and duct velocity profile causes a tremendous difference in the observed flow patterns and cleaning efficiency. The percentage of fluid removed from a cavity can be increased as Grashof number, H/D and cavity aspect ratio increase. In contrast to the results without the effect of mixed convection, Couette flow at higher value of

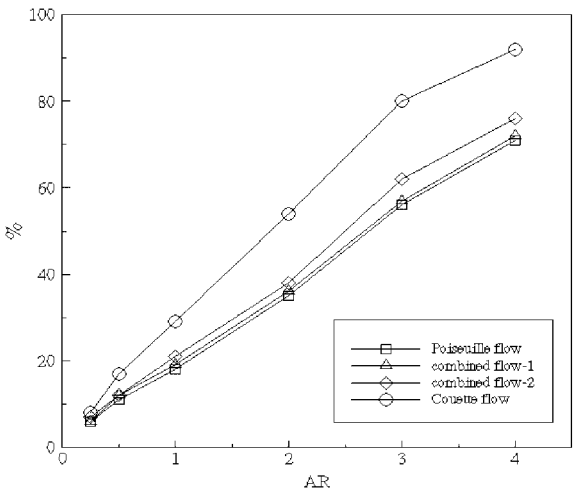

Figure 15. Percentage of markers removed from the cavity for varied velocity profiles of duct flow, at $Gr = 2000$ and $Re = 50$.

Gr becomes more effective than Poiseuille flow in further purging of contaminated fluid from a cavity. It is interesting to note that for the values of *Gr* higher than 2000 the steady-state result with Couette flow could not be obtained since oscillatory behaviour was observed. For Poiseuille flow, this phenomena does not occur until *Gr* greater than 4000.

REFERENCES

1. Jennings WG, Mckillop AA, Luick JB. Circulating cleaning. *Journal of Diary Science* 1957; **40**:1471–1479.
2. Jennings WG. Theory and practice of hard surface cleaning. *Advances in Food Research* 1965; **14**:325–458.
3. Corrieu D. State of the art of cleaning surfaces. In *Fundamentals of Applications of Surface Phenomena Conference*, Hallstrom B (ed.), 1981; 90–114.
4. Takematsu M. Slow viscous flow past a cavity. *Journal of the Physical Society of Japan* 1966; **21**:1816–1821.
5. Taneda S. Visualization of separating Stokes flows. *Journal of the Physical Society of Japan* 1979; **46**:1935–1942.
6. Shen C, Floryan JM. Low Reynolds number flow over cavities. *Physics of Fluids* 1985; **28**:3191–3202.
7. Higdon JL. Stokes flow in arbitrary two-dimensional domains: shear flow over ridges and cavities. *Journal of Fluid Mechanics* 1985; **159**:195–226.
8. Chang HN, Ryn HW, Park DH, Park YS. Effect of external laminar channel flow on mass transfer in a cavity. *International Journal of Heat and Mass Transfer* 1987; **30**:2137–2149.
9. Pozrikidis C. Shear flow over a plane wall with an axisymmetric cavity or a circular orifice of finite thickness. *Physics of Fluids* 1994; **6**:68–79.
10. Fang LC, Nicolaou D, Cleaver JW. Transient removal of a contaminated fluid from a cavity. *International Journal of Heat and Fluid Flow* 1999; **20**:605–613.
11. Fang LC, Nicolaou D, Cleaver JW. Channel flow over a cavity containing a miscible heavier liquid. *International Journal of Transport Phenomena* 2003; **5**:47–63.
12. Chilukrishna R, Middleman S. Circulation, diffusion, and reaction within a liquid trapped in a cavity. *Chemical Engineering Communications* 1983; **22**:127–138.
13. Mehta UB, Lavan Z. Flow in a two-dimensional channel with a rectangular cavity. *Transactions of ASME, Journal of Applied Mechanics* 1969; **36**:897–901.
14. O'Brien V. Closed streamlines associated with channel flow over a cavity. *Physics of Fluids* 1972; **15**:2089–2097.
15. Mickaily ES, Middleman S, Allen M. Viscous flow over periodic surfaces. *Chemical Engineering Communications* 1992; **117**:401–414.

16. Oberkampf WL, Crow LI. Numerical study of the velocity and temperature fields in a flow-through reservoir. *ASME Journal of Heat Transfer* 1976; **98**:353–359.
17. Sparrow EM, Samie F. Interaction between a stream which passes through an enclosure and nature convection within the enclosure. *International Journal of Heat and Mass Transfer* 1982; **25**:1489–1502.
18. Cha CK, Jaluria Y. Effect of thermal buoyancy on the recirculating flow in a solar pond for energy extraction and heat rejection. *ASME Journal of Solar Energy Engineering* 1984; **25**:428–437.
19. Oosthuizen PH, Paul JT. Mixed convection heat transfer in a cavity, in fundamentals of forced and mixed convection. *ASME HTD* 1990; **42**:159–169.
20. Papanicolaou E, Jaluria Y. Mixed convection from an isolated heat source in a rectangular enclosure. *Numerical Heat Transfer A* 1990; **18**:427–461.
21. Fang LC. Effect of mixed convection on efficiency of transient hydrodynamic removal of a contaminant from a cavity. *International Journal of Heat and Mass Transfer* 2003; **46**:2039–2049.
22. Torrance K, Davis R, Eike K, Gill P, Gutman D, Hsui A, Lyons S, Zien H. Cavity flows driven by buoyancy and shear. *Journal of Fluid Mechanics* 1971; **51**:221–231.
23. Harlow FH, Welch JE. Numerical calculation of time-dependent viscous incompressible fluid with free surface. *Physics of Fluids* 1965; **8**:2182–2189.
24. Miyata H, Nishimura S. Finite-difference simulation of nonlinear ship waves. *Journal of Fluid Mechanics* 1982; **157**:327–357.
25. Chorin AJ. Numerical solution of the Navier–Stokes equations. *Mathematics of Computation* 1968; **22**:745–762.
26. Viecelli JA. A computing method for incompressible flows bounded by moving walls. *Journal of Computational Physics* 1971; **8**:119–143.
27. Kuo CH, Sharif MAR, Scheriber WC. Numerical Experiments on the simulation of Benard convection using Marker and Cell method. *Chemical Engineering Communications* 1994; **127**:1–21.
28. Welch JE, Harlow FH, Shannon JP, Daly BJ. The MAC method—a computing technique for solving viscous, incompressible, transient fluid-flow problems involving a free surface. *Los Alamos Scientific Laboratory Report*, LA-3425, Los Alamos, 1966.

